CrossMark

ORIGINAL PAPER

Facile Biosynthesis of Silver Nanoparticles Using *Descurainia sophia* and Evaluation of Their Antibacterial and Antifungal Properties

Mehrdad Khatami[1] · **Rasoul Mehnipor**[2] ·
Mohammad Hossein Sobhani Poor[1] ·
Gholamreza Salehi Jouzani[3]

Abstract The objective of the present study was to evaluate efficiency of silver nanoparticles (Ag-NPs) biosynthesis using *Descurainia sophia* as a novel biological resource. The resulting synthesized Ag-NPs were characterized using UV visible spectroscopy, X-ray diffraction, transmission electron microscopy and dynamic light scattering (DLS). The UV–Vis spectra gave surface plasmon resonance at ~ 420 nm. TEM images revealed formation spherical shaped Ag-NPs with size ranged from to 1–35 nm. DLS confirmed uniformity of the synthesized Ag-NPs with an average size of ~ 30 nm. Following, the antibacterial and antifungal activities of the synthesized Ag-NPs were investigated. The concentration 25 μg/ml of the Ag-NPs showed maximum inhibitory effect on mycelium growth of *Rhizoctonia solani* (More than 86 % inhibition), followed by 15 μg/ml (55 % inhibition) and 10 μg/ml (63 % inhibition). The minimum inhibitory concentration and minimum bactericidal concentration of Ag-NPs

✉ Mehrdad Khatami
   mehrdad7khatami@gmail.com; M.Khatami@amubam.ac.ir

   Rasoul Mehnipor
   Rasoul.mehnipor@gmail.com

   Mohammad Hossein Sobhani Poor
   sobhani6557@yahoo.com

   Gholamreza Salehi Jouzani
   gsalehi@abrii.ac.ir

[1]   Bam University of Medical Sciences, Bam, Iran

[2]   Blood Transfusion Research Center, High Institute for Research and Education in Transfusion Medicine, Tehran, Iran

[3]   Microbial Biotechnology Department, Biotechnology Research Institute of Iran (ABRII), AREO, P.O.Box 31535-1897, Karaj, Iran

against *Agrobacterium tumefaciens* (strain GV3850) and *A, rhizogenes* (strain 15843) were 4 and 8 µg/ml, respectively. The Ag-NPs were stable in vitro for 3 months without any precipitation or decrease of antifungal effects. Finally, it could be concluded that *D. sophia* can be used as an effective method for biosynthesis of nanoparticles, especially Ag-NPs.

Introduction

In the recent years, efficient nano-materials and nanoparticles synthesis has attracted a great deal of attention, because of their valuable properties making them ideal for the production of therapeutics, antimicrobials, sensitive diagnostics (sensor technology), membranes, catalysts, photonics, and optoelectronics [1–3]. Resistance to commercially available antimicrobial agents by pathogenic fungi and bacteria has been increasing at an alarming rate and has become a serious problem [4, 5]. There is a pressing need to search for new antifungal agents. Silver nanoparticles (Ag-NPs) are proved to have high potential antimicrobial, antiplasmodial, antifungal and properties, so recently, they have been used for controlling harmful microorganisms such as bacteria, molds, yeasts and viruses [6, 7].

Different routes have been developed to synthesize Ag-NPs while striving to consume less energy, increase efficiency and more importantly to develop eco-friendly procedures [1, 2, 8, 9]. One of such methods is the production of Ag-NPs using biological systems, such as bacteria [1, 10], fungi [11], algae [12, 13] and plants [14, 15].

Previously, it has been shown that different biomolecules present in plants extracts can reduce metal ions to nanoparticles in a single-step green synthesis process. Extracts of different tissues of a diverse range of species have been successfully used in making Ag-NPs [16–20]. This process is quite rapid, readily conducted at room temperature and pressure, easily scaled up, and more importantly is environmental friendly. The reducing agents involved include the various water soluble metabolites (e.g. alkaloids, phenolic compounds, terpenoids) and co-enzymes [18].

Descurainia sophia (Flixweed) is an annual dicot belonging to family Brassi-caceae (Cruciferae), which its seeds have been used in folk medicines for the treatment of throat diseases, measles and smallpox in the middle Asia [21, 22]. The seeds of this plant contain various types of secondary metabolites, such as cardiac glycosides, flavonoids, lactones, lipids, sulfur glycoside, nor-lignan, and coumarins with biological effects [22–24]. So, the objective of the present study was to evaluate possibility of Ag-NPs biosynthesis using *D. sophia* germinating seeds extract, and to evaluate antimicrobial properties of synthesized Ag-NPs against fungus *R. solani*, and also against *A. tumefaciens* and *A. rhizogenes*. To the best of our knowledge, this study is the first report of Ag-NPs biosynthesis using the flixweed.

Materials and Methods

Preparation of Extract

The surface of *D. sophia* seeds were disinfected using sodium hypochlorite and 70 % alcohol, then imbibed in deionized water (DIW) (1 g dry weight/10 ml DIW) [25]. After being incubated at 26 °C for 48 h in dark, seeds were removed from the soaking medium. The supernatant phase was collected and centrifuged at 4500 rpm for 10 min to separate the liquid fraction from any large insoluble particles, and filtered by Whatman filter paper No. 40. During the experiment, pH was 4.5 as previously described [14].

Biosynthesis of Ag-NPs

Silver nitrate ($AgNO_3$) was used as the source of the synthesis of Ag-NPs (Merck, Germany). Fifteen ml of the obtained seed extract was diluted by 30 ml sterile DIW and added to 4 mM $AgNO_3$ to reduce Ag^+ to Ag^0. The samples were stored at 28 °C in the dark.

Specification of Ag-NPs

UV Visible Spectrophotometry Analysis

The formation of Ag-NPs was monitored by using UV visible spectrophotometry, Scan Drop-type, Analytic Jena, Germany. Absorption wavelength was studied range between 300 and 600 nm.

XRD Analysis

The reaction mixture (extract + Ag-NPs) was centrifuged at 14,000 rpm for 15 min by redispersion of Ag-NPs sedimentation into deionized water for three times. The sedimentation was transferred in incubator (60 °C) for drying. The resulting Ag-NPs powder used for XRD measurement.

TEM Analysis

Transmission Electron Microscopy (Carl ZIESS Microscope, Germany (80 KB) was used to determine the size, shape and distribution of Ag-NPs. To prepare the sample, 10 ml of the sample was ultrasonicated for 5 min, then poured onto a grid with a carbon film and air-dried at room temperature without the use of heat [26].

Dynamic Light Scattering (DLS)

The size of the distributed Ag-NPs were measured by using the principle of dynamic light scattering (DLS) technique made in a Malvern Zetasizer Nano series compact scattering spectrometer [14].

Evaluation of Antifungal Activity of Ag-NPs

Agar diffusion method was used to determine the antifungal activity of synthesized Ag-NPs against *R. solani*. Ag-NPs with different concentrations were poured into growth media prior to plating in a Petri dish (75 × 15 mm). PDA medium containing different concentrations (10, 15 and 25 μg/ml, Ag-NPs) was incubated at room temperature. After 48 h incubation, agar plugs of uniform size (diameter, 6 mm) containing fungi were inoculated simultaneously at the center of each Petri dish containing Ag-NPs, and incubated at 28 °C for 3 days in an incubator. When control fungus completely covered the entire surface of the medium, the mean radius of fungal growth in the medium was measured [14]. The experiments were performed in triplicate. The following formula was used for assessing the zone of inhibition rate.

$$\text{Inhibition rate } (\%) = \frac{R - r}{R}$$

"R" is the radius of mycelium growth of the control sample and "r" radius of fungal mycelium growth in samples treated with nanoparticles. Data with SAS statistical analysis was performed by Duncan's test.

## Evaluation of Antibacterial Activity of Ag-NPs

The susceptibility of *A. tumefaciens* (strain GV3850) and *A. rhizogenes* (strain 15843) to the Ag-NPs were studied using the standard method of the serial dilution preparation in agar and broth medium containing Ag-NPs to determining the relative minimum concentration that inhibits the bacteria growth [27, 28]. The strains were grown overnight in 50 mL sterile Erlenmeyer flasks containing 25 mL of LB containing rifampicin (50 mg/l). The bacterial cell density was then adjusted to CFU/mL 1.5×10^8 using fresh LB medium. The Ag-NPs were added to the bacterial cells in different final concentrations, including 0, 1, 2, 4, 8, 16, 32, 64, 128 and 256 μg/ml. The medium containing bacteria without any Ag-NPs was used as control. Then, the inoculated media were transferred to tubes and plates (NA medium) containing certain concentrations of Ag-NPs, and incubated in 28 °C for 48 h. All treatments were performed in triplicates. After 48 h, the minimum inhibitory concentration (MIC) and the minimum bactericidal concentration (MBC) of each treatment was measured, as previously described [28]. The MIC value corresponded to the concentration that inhibited 99 % of bacterial growth, and the MBC value corresponded to the concentration where 100 % of the bacterial growth was inhibited, compared to the control [28].

Results and Discussion

Visual Observation

Reduction of Ag^+ to Ag^0 was confirmed by color change of the reaction mixture from colorless to brown (Fig. 1). This color change is morphological indicator to

Fig. 1 The color change of seed exudates upon the formation of silver nanoparticles, **a** *Descurainia sophia* extract (control), **b** 4 mM AgNO₃
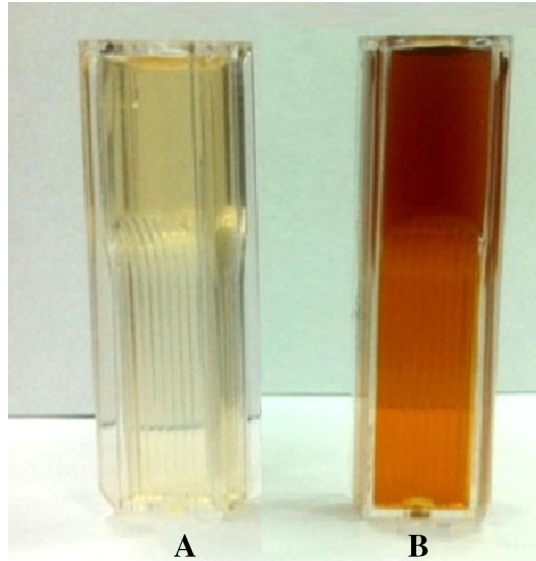
detect the synthesis of Ag-NPs. Color of silver colloid is attributed to surface Plasmon resonance arising due to the collective oscillation of free conduction electrons induced by an interacting electromagnetic field [29].

UV Visible Spectrophotometer

The absorption peak of exudates treated with silver nitrate in the range of ~420 nm indicates the formation of Ag-NPs (Fig. 2). Spectroscopy spectrum of the reaction
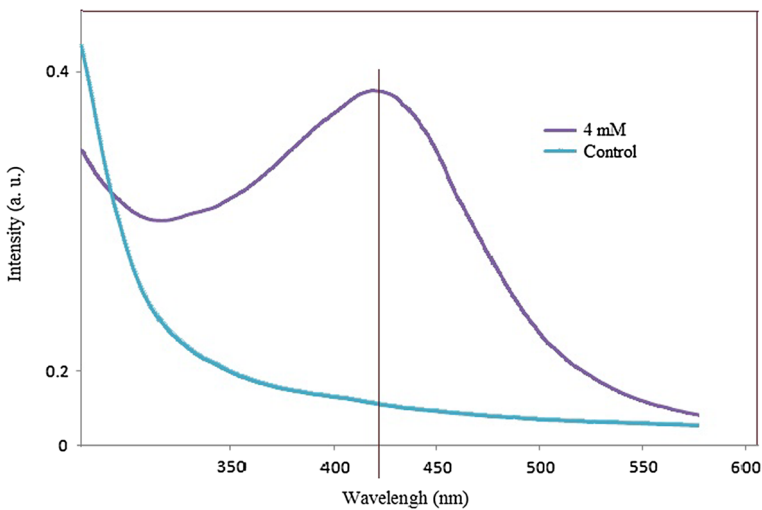
Fig. 2 UV–Vis absorption spectrum of the silver nanoparticles synthesized by treating 4 mM AgNO₃
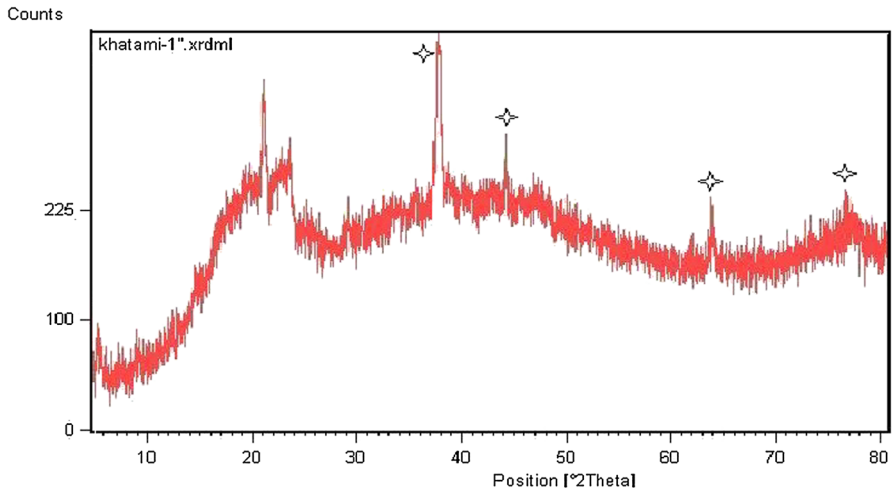
Fig. 3 X-ray diffraction pattern of silver nanoparticles synthesized using *Descurainia sophia*

mixture containing exudates treated with silver nitrate was measured at concentration 4 mM (Fig. 2).

XRD Results

Sharp peaks (✧) were observed in XRD pattern (Fig. 3) of Ag-NPs powder at 2θ values of 38, 44, 64 and 77 which corresponding respectively to 111, 200, 220 and 311 planes of FCC structure Ag-NPs.

TEM Analysis

TEM images of Ag-NPs at various magnifications confirmed spherical shapes of Ag-NPs (Fig. 4) with most clearly apparent diameter size from 1 to 35 nm (Fig. 5).
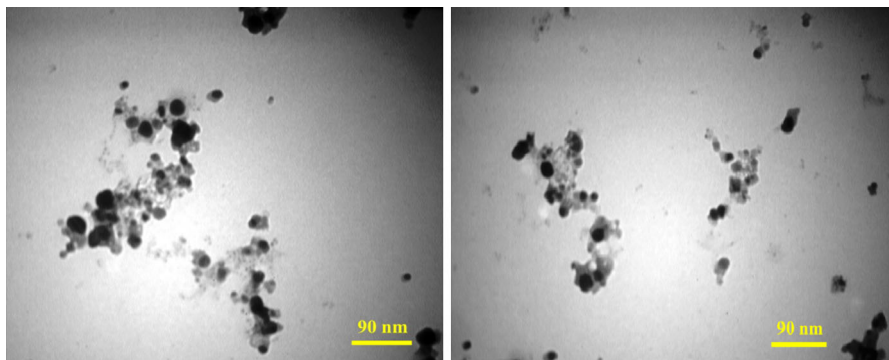

Fig. 4 TEM images of the synthesized silver nanoparticles in *different scales*
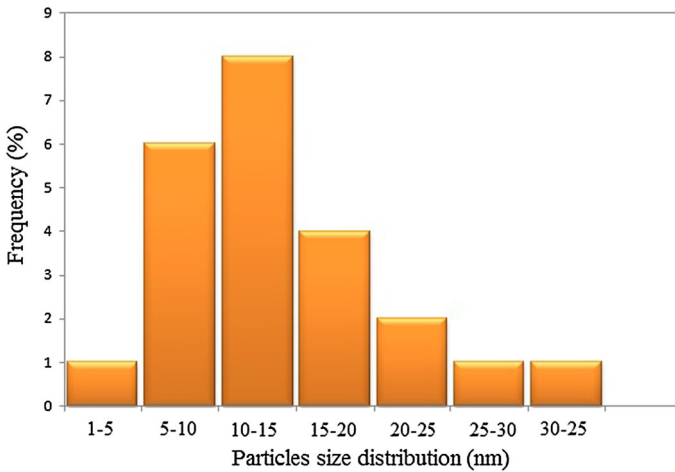
Fig. 5 The histogram of the particle size distribution of the biosynthesized silver nanoparticles

Dynamic Light Scattering (DLS)

DLS studies showed that the Ag-NPs were synthesized with a uniform distribution and an average particle size ∼30 nm (Fig. 6a). The average particle size of Ag-NPs obtained through DLS is normally larger than the TEM results (15 nm). TEM images gives the 'true diameter' of the particles which considers only the metallic core on an ensemble average, where as DLS provides the hydrodynamic diameter, including the ligand shell and determines the hydrodynamic size (Fig. 6b) [30, 31]. Ag-NPs were stable at 28 °C in vitro for 3 months without any precipitation or decreased production of antifungal effect.

Previously, it has been showed that the reducing agents present some bioresources, involved in nanoparticles production, include the various water soluble metabolites (e.g. alkaloids, phenolic compounds, terpenoids) and co-enzymes [18]. Extracts of different tissues of a diverse range of species have been successfully used in making Ag-NPs [16–19, 32, 33]. In the present study, for the first time *D. sophia* was used for production of Ag-NPs, as previously, it has been confirmed that seeds of this plant contain various types of water soluble secondary metabolites, such as glycosides, flavonoids, lactones, sulfur glycosides, and coumarins and also coenzymes which may be act as reducing agents for this purpose [22–24]. The UV visible spectrophotometer, TEM and DLS analysis showed that the seed extracts could efficiently reduce Ag ions to Ag^0, and therefore, flixweed can be used an efficient source for NPs production.

Antifungal and Antibacterial Activities of the Synthesized Ag-NPs

Inhibitory effects of different concentrations of the produced Ag-NPs (0, 10, 15 and 25 µg/ml) on *R. solani* growth were studied. The results showed significant antifungal activity (P < 0.05) of the synthesized Ag-NPs on the mycelium growth
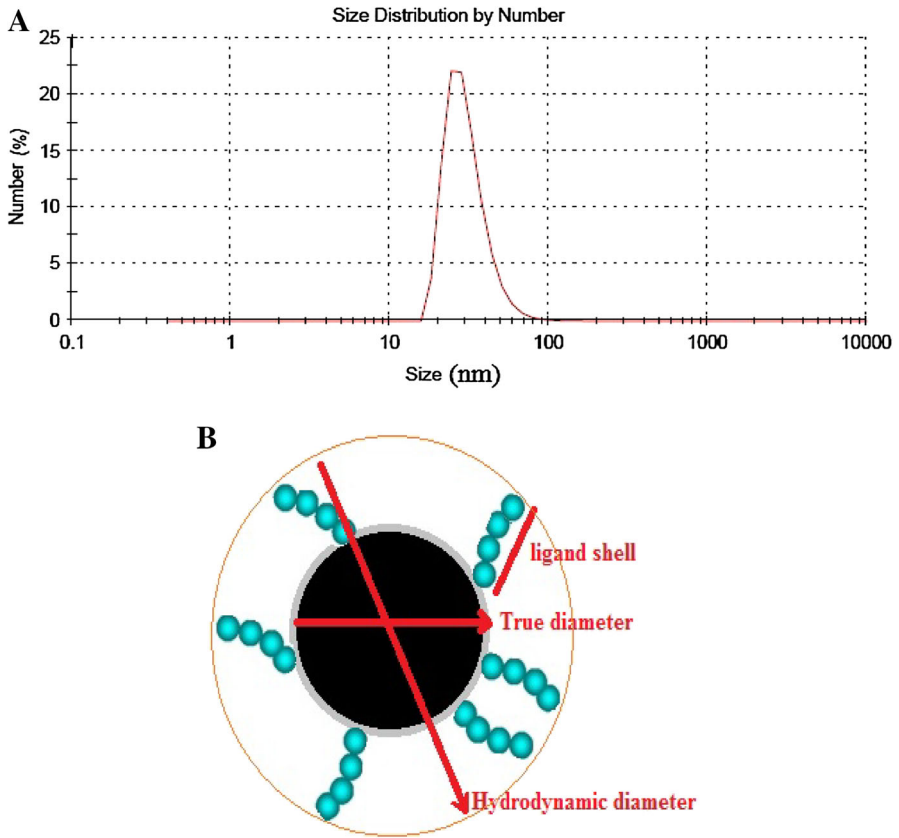
Fig. 6 Size distribution of silver nanoparticles (**a**), and true diameter, hydrodynamic diameter and ligand shell of the synthesized silver nanoparticles (**b**) using DLS
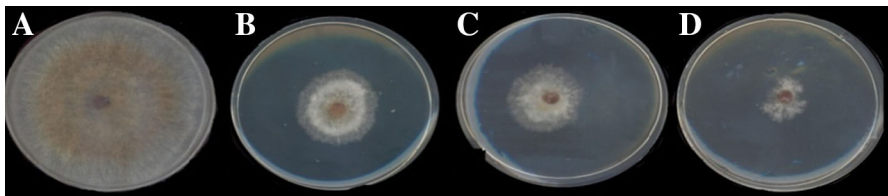

Fig. 7 *Rhizoctonia solani* mycelium growth on PDA medium containing **a** control, **b** 10, **c** 15 and **d** 25 μg/ml silver nanoparticles

of the fungus. The concentration 25 μg/ml of the synthesized Ag-NPs showed maximum inhibitory effect on mycelium growth (More than 86 % inhibition), followed by 15 μg/ml (55 % inhibition) and 10 μg/ml (63 % inhibition) (Fig. 7).

The results clearly showed that the zone of inhibition of nanoparticles strongly depends on their concentration, and greatly increases by increasing the Ag-NPs concentration in the medium. Previously, different studies confirmed that Ag-NPs show high antifungal activities against various types of pathogens, such as *Alternaria alternata* [29, 34–36], *Alternaria solani* [37], *Aspergillus flavus, A. fumigatus, A. versicolor, A. niger, Botrytis cinerea* [29], *Colletotrichum gloeosporioides* [38], *Curvularia lunata* [29], *Fusarium solani* [34, 35], *F. verticillioides* [34], *F. oxysporum* [34, 35], *F.udum* [36], *Macrophomina phaseolina* [29, 36], *Sclerotinia sclerotiorum* [29, 39], *S. minor* [39], and *Malassezia furfur* (*Pityrosporum ovale*), a lipophilic fungus. In addition, it has been proved that Ag-NPs have high antifungal activity against *R. solani* [29, 35, 39]. Shanmugaiah et al. showed that antifungal activities of Ag-NPs is highly concentration depended and concentration 7 ppm showed the highest inhibition activity (more than 75 %) which is highly in accordance with our results [36]. Shanmugaiah et al. showed that the MIC value of synthesised Ag-NPs against *R. solani* was 10 µl/ml which was in accordance with our results as the antifungal activity was continuously increased by increasing the Ag-NPs from 10 to 25 µl/ml. In another study, also it was confirmed that effective concentration Ag-NPs inhibiting 50 % of *R. solani* growth was 9.2 µl/ml and its inhibitory effect is concentration depended [35]. Due to the significant antifungal effect of synthesized Ag-NPs, it is suggested these Ag-NPs are used as a powerful antifungal agent.

Also, previously it has been confirmed that Ag-NPs show high antibacterial activities against different types of bacteria (human pathogens), such as *Escherichia coli* [40], *Bacillus cereus* [41], *Bacillus subtilis* [41], *Pseudomonas aeruginosa* [42, 43], *Staphylococcus aureus* [41, 42], *Vibrio cholera* [40], *Enterococcus faecalis, Staphylococcus aureus, Staphylococcus epidermidis, Staphylococcus aureus, Enterococcus faecium* and *Klebsiella pneumoniae* [43]. In the present study, for the first time antimicrobial activity od Ag-NPs was evaluated against *A. tumefaciens* and *A. rhizogenes*. The antibacterial activities of the synthesized Ag-NPs were evaluated on *A. tumefaciens* and *A. rhizogenes* strains in both LB and NA media. The results of dilution broth test showed that the MIC and MBC values of Ag-NPs against both *A. tumefaciens* and *A. rhizogenes* were 4 and 8 µg/mL, respectively (Table 1), while both MIC and MBC values of Ag-NPs calculated by

Table 1 The antibacterial activities (MIC and MBC) of different concentrations of the synthesized Ag-NPs on *A. tumefaciens* and *A. rhizogenes* in micro-dillution system

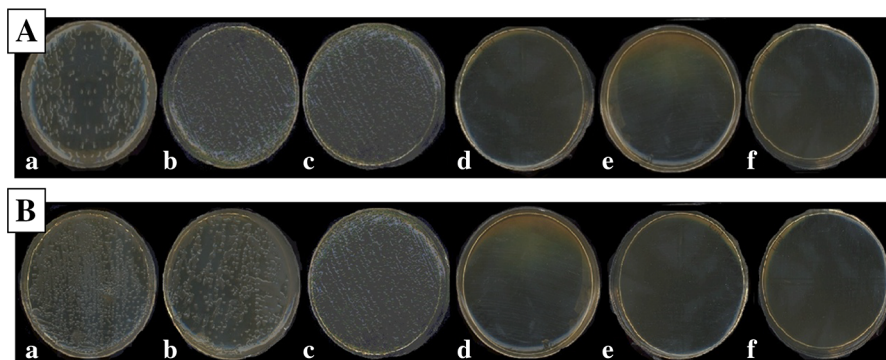| Bacterial strains	Ag-NPs (µg/mL)									
	0	1	2	4	84	16	32	64	128	256
Agrobacterium rhizogenes (15823)	+	+	+	–*	–**	–	–	–	–	–
A. tumefaciens (GV3850)	+	+	+	–*	–**	–	–	–	–	–

– no growth, + growth, * MIC, ** MBC

Fig. 8 The antibacterial activities of different concentrations of the synthesized Ag-NPs on *Agrobacterium tumefaciens* and *Agrobacterium rhizogenes* in LB agar. **a** 0 μg/ml, **b** 2 μg/ml, **c** 4 μg/ml, **d** 8 μg/ml, **e** 16 μg/ml and **f** 32 μg/ml

agar dilution method against *A. tumefaciens* and *A. rhizogenes* were 8 μg/mL (Fig. 8).

These results were similar to the results of other researchers who showed that antibacterial activity of Ag-NPs is dependent on the size and concentration of silver particles, and a very low concentration of silver (2–10 μg/mL Ag) give antibacterial performance [40, 42–46]. Also, totally these results are in accordance to the previous studies which have confirmed high antibacterial, antifungal and antiplasmodial properties of Ag-NPs [19]. Recently, Aminedi et al. showed that the TiO_2 nanorods and nanotubes has high antimicrobial effects against *A. tumefaciens*, and this antimicrobial activity increase by reducing the size and increasing specific surface of the particles [47]. In other work, to offer an insight into the toxicity of nanomaterials on the growth of *E. coli*, *B. subtilis* and *A. tumefaciens* were exposed to Au-NPs, Ag-NPs, Fe-NPs and fullerene (C_{60}) [48]. It was shown that Ag-NPs induced the highest toxicity on these three bacteria. Le et al. investigated the cytotoxicity, genotoxicity, and growth inhibition effects of four different inorganic nanoparticles (NPs) such as aluminum (Al), iron (Fe), nickel (Ni), and zinc (Zn) in single and mixed systems on *Agrobacterium* sp [49]. The results showed that the mixing system enhance the antibacterial activities of the NPs. Our results confirmed that the Ag-NPs are capable of showing high antimicrobial activity against Agrobacterium, which is in accordance with the previous works [47–49].

Conclusion

Based on the results of the present study, it could be concluded that DGSE can be used as an effective method for biosynthesis of Ag-NPs. The produced Ag-NPs had a high uniformity, normal distribution and high stability, spherical in shape and 1–35 nm in size. The biosynthesized Ag-NPs showed high and fast antifungal effects against *R. solani* and antimicrobial activity against *A. tumefaciens* and *A. rhizogenes*.

Compliance with Ethical Standards

Conflict of interest The authors declare that they have no conflict of interest.

References

1. M. M. Juibari, S. Abbasalizadeh, G. S. Jouzani, and M. Noruzi (2011). *Mater. Lett.* **65**, (6), 1014–1017.
2. M. Juibari, L. Yeganeh, S. Abbasalizadeh, R. Azarbaijani, S. Mousavi, M. Tabatabaei, et al. (2015). *BioNanoScience* **5**, (4), 233–241.
3. M. S. Nejad, M. Khatami, and G. H. S. Bonjar (2015). *Nanomed. J.* **2**, (3), 233–238.
4. J. Zhang, Y. P. Chen, K. P. Miller, M. S. Ganewatta, M. Bam, Y. Yan, et al. (2014). *J. Am. Chem. Soc.* **136**, (13), 4873–4876.
5. G. D. Wright (2005). *Adv. Drug Deliv. Rev.* **57**, (10), 1451–1470.
6. R. Bryaskova, D. Pencheva, S. Nikolov, and T. Kantardjiev (2011). *J. Chem. Biol.* **4**, (4), 185–191.
7. G. Franci, A. Falanga, S. Galdiero, L. Palomba, M. Rai, G. Morelli, et al. (2015). *Molecules* **20**, (5), 8856.
8. B. G. Anand, C. K. N. Thomas, S. Prakash, and C. S. Kumar (2015). *Biocatal. Agric. Biotechnol.* **4**, (2), 150–157.
9. S. A. Moon, B. K. Salunke, B. Alkotaini, E. Sathiyamoorthi, B. S. Kim (2015) *IET Nanobiotechnol.* **9**(4), 220–225. Available from: http://digital-library.theiet.org/content/journals/10.1049/iet-nbt.2014.0051.
10. V. Ramalingam, R. Rajaram, C. PremKumar, P. Santhanam, P. Dhinesh, S. Vinothkumar, et al. (2014). *J. Basic Microbiol.* **54**, (9), 928–936.
11. A. O. de Souza and A. G. Rodrigues *Biosynthesis of Silver Nanoparticles by Fungi* (Wiley, Hoboken, 2014).
12. Z. Salari, F. Danafar, S. Dabaghi, S. A. Ataei (2016) J. Saudi Chem. Soc.
13. S. Sinha, D. Paul, N. Halder, D. Sengupta, and S. Patra (2015). *Nanoscience* **5**, (6), 703–709.
14. M. Khatami, S. Pourseyedi, M. Khatami, H. Hamidi, M. Zaeifi, and L. Soltani (2015). *Bioresour. Bioprocess.* **2**, (19), 1–7.
15. A. K. Mittal, J. Bhaumik, S. Kumar, and U. C. Banerjee (2014). *J. Colloid Interface Sci.* **415**, 39–47.
16. S. Iravani (2011). *Green Chem.* **13**, (10), 2638–2650.
17. M. Vijayakumar, K. Priya, F. T. Nancy, A. Noorlidah, and A. B. A. Ahmed (2013). *Ind. Crops Prod.* **41**, 235–240.
18. A. K. Mittal, Y. Chisti, and U. C. Banerjee (2013). *Biotechnol. Adv.* **31**, (2), 346–356.
19. C. Panneerselvam, K. Murugan, and D. Amerasan (2015). *Adv. Mater. Res.* **1086**, 11–30.
20. C. Keat, A. Aziz, A. Eid, and N. Elmarzugi (2015). *Bioresour. Bioprocess.* **2**, (1), 47.
21. A. Mokhtassi-Bidgoli, M. AghaAlikhani, M. Nassiri-Mahallati, E. Zand, J. L. Gonzalez-Andujar, and A. Azari (2013). *Ind. Crops Prod.* **44**, 583–592.
22. N. P. Bekker, N. T. Ul'chenko, and A. I. Glushenkova (2005). *Chem. Nat. Compd.* **41**, (3), 346–347.
23. X. Zhou, L. Tang, H. Wu, G. Zhou, T. Wang, Z. Kou, et al. (2015). *J. Pharm. Biomed. Anal.* **111**, 1–6.
24. Y. Lee, N. Kim, H. Kim, J.-M. Yi, S.-M. Oh, O.-S. Bang, et al. (2013). *Arch. Pharm. Res.* **36**, (5), 536–541.
25. M. Khatami, M. S. Nejad, and S. Pourseyedi (2015). *Int. J. Nanosci. Nanotechnol.* **11**, (4), 279–287.
26. M. Khatami and S. Pourseyedi (2015). *IET Nanobiotechnol.* **9**, (4), 184–190.
27. C. A. Rotilie, R. J. Fass, R. B. Prior, and R. L. Perkins (1975). *Antimicrob. Agents Chemother.* **7**, (3), 311–315.
28. G. Wu, Q. Yang, M. Long, L. Guo, B. Li, Y. Meng, et al. (2015). *J Antibiot.* **68**, (11), 661–665.
29. C. Krishnaraj, R. Ramachandran, K. Mohan, and P. T. Kalaichelvan (2012). *Spectrochim. Acta Part A* **93**, 95–99.
30. J. Lim, S. Yeap, H. Che, and S. Low (2013). *Nanoscale Res. Lett.* **8**, (1), 381.

31. R. Pecora (eds) *Dynamic Light Scattering: With Applications to Chemistry, Biology, and Physics. Physics DBo* (Dover Publications, Mineola, 2000).

32. K. Shameli, M. Bin Ahmad, E. A. Jaffar Al-Mulla, N. A. Ibrahim, P. Shabanzadeh, A. Rustaiyan, et al. (2012). *Molecules* **17**, (7), 8506.

33. J. Song and B. Kim (2009). *Bioprocess Biosyst Eng.* **32**, (1), 79–84.

34. Y. Xu, C. Gao, X. Li, Y. He, L. Zhou, G. Pang, et al. (2013). *J. Ocul. Pharmacol. Ther.* **29**, (2), 270–274.

35. A. Abdel-Megeed, et al. (2015). *J. Environ. Biol.* **36**, (4), 1–5.

36. V. Shanmugaiah, H. Harikrishnan, N. S. Al-Harbi, K. Shine, J. M. Khaled, N. Balasubramanian, et al. (2015). *Dig. J. Nanomater. Biostruct.* **10**, 179–187.

37. A. W. A. Ismail, N. M. Sidkey, R. A. Arafa, R. M. Fathy, and A. I. El-Batal (2016). *Brit. Biotechnol. J.* **12**, (3), 1–11.

38. C. Shanmugam, D. Gunasekaran, N. Duraisamy, R. Nagappan, and K. Krishnan (2015). *RSC Adv.* **5**, (87), 71174–71182.

39. J. S. Min, et al. (2009). *Plant Pathol. J.* **25**, (4), 376–380.

40. C. Krishnaraj, E. G. Jagan, S. Rajasekar, P. Selvakumar, P. T. Kalaichelvan, and N. Mohan (2010). *Colloids Surf. B* **76**, (1), 50–56.

41. U. B. Jagtap and A. Bapat (2013). *Ind. Crops Prod.* **46**, 132–137.

42. M. Guzman, J. Dille, and S. Godet (2012). *Nanomedicine* **8**, (1), 37–45.

43. L. Kvitek, A. Panáček, J. Soukupova, M. Kolar, R. Vecerova, R. Prucek, et al. (2008). *J. Phys. Chem. C* **112**, (15), 5825–5834.

44. A. Panáček, L. Kvítek, R. Prucek, M. Kolář, R. Večeřová, N. Pizúrová, et al. (2006). *J. Phys. Chem. B* **110**, (33), 16248–16253.

45. J. P. Ruparelia, A. K. Chatterjee, S. P. Duttagupta, and S. Mukherji (2008). *Acta biomater.* **4**, (3), 707–716.

46. I. Sondi and B. Salopek-Sondi (2004). *J. Colloid Interface Sci.* **275**, (1), 177–182.

47. R. Aminedi, G. Wadhwa, N. Das, and B. Pal (2013). *Environ. Sci. Pollut. Res.* **20**, (9), 6521–6530.

48. C. Wang, L. Wang, Y. Wang, Y. Liang, and J. Zhang (2012). *Environ. Earth Sci.* **65**, (6), 1643–1649.

49. T. Le, K. Murugesan, E.-J. Kim, and Y.-S. Chang (2014). *Biodegradation* **25**, (5), 655–668.